



Estimation of the drop modulus using the brittleness index of intact rock and geological strength index of rock mass, case studies: Nosoud and Zagros tunnels in Iran

M. Soleiman Dehkordi¹ · H. A. Lazemi¹ · H. R. SaeedModaghegh¹

Received: 2 November 2018 / Accepted: 22 February 2019 / Published online: 5 April 2019
© Springer Nature Switzerland AG 2019

Abstract

The drop modulus is defined as the slope for the softening stage of the stress–strain curve of rock mass. Estimation of the mentioned parameter is very difficult because it is related to many parameters such as intact rock properties, quality of rock mass, confinement stress and etc. In this study, based on the actual collected data from Nosoud and Zagros tunnels in Iran, new empirical equations to predict the drop modulus of rock mass using the brittleness indexes is proposed. The results show that there is a direct relation between both parameters and the best correlation between them is achieved using the Altindag's brittleness index, BI3, to estimate the drop modulus. Finally, the relation between the drop modulus with the brittleness index of intact rock and geological strength Index of rock mass is estimated and a new equation to estimate the drop modulus using both mentioned parameters is proposed.

Keywords Drop modulus · Brittleness index · GSI · Strain softening behavior

Introduction

The area under stress–strain curve is called strain energy. In predicting the in situ performance of an excavation, it would be expected that excavating underground spaces induced local response in surrounding rock mass of excavations that it would depend on both the volume of rock subject to induced stress and the magnitude and distribution of the stress components in the affected volume. They are incorporated in the static strain energy increase (ΔW_s). For the elastic analysis, the increase in static strain energy was equivalent to the energy released by excavation (W_r). However, local rock fracture which occurs around excavation consumes some of the released energy. If a fracture does not occur, $\Delta W_s = W_r$. If fracture occurs, the rock fracture energy, W_f , reduces the stored energy, such that $W_r = \Delta W_s + W_f$. Ultimately, in the case of extensive rock fracture, all the released energy may be consumed in rock disintegration (Brady and Brown 2005). The energy balance conditions of the rock

mass in post-failure regions was considered by Tarasov and Potvin (2013). The energy in the post-peak stage can be classified into three types according to Fig. 1: the elastic energy (colored green) is the stored and released elastic energy in the material during loading and failure, the rupture energy represented by the orange areas is the shear rupture energy under confinement, and the additional energy (in yellow) represents the absorbed or released energy during failure (Tarasov and Potvin 2013 and Decheng; Zhang et al. 2016).

The failure process can be classified into two types according to the value of drop modulus (Wawersik and Fairhurst 1970). In Class I failure mode, the material continuously deforms, absorbing extra energy (yellow areas) during the load application to progress the failure process, while in Class II failure mode, the failure is characterized by strain recovery and release of energy, which can be seen as self-sustaining (Decheng Zhang et al. 2016). It was shown in Fig. 2.

Hoek and Brown (1997) suggested guidelines to estimate the post-failure behavior types of rock mass according to rock mass quality. These guidelines are based on rock types (Hoek and Brown 1997):

✉ M. Soleiman Dehkordi
Mohsen.soleiman@gmail.com

¹ Department of Civil Engineering, Bafgh Branch, Islamic Azad University, Bafgh, Iran

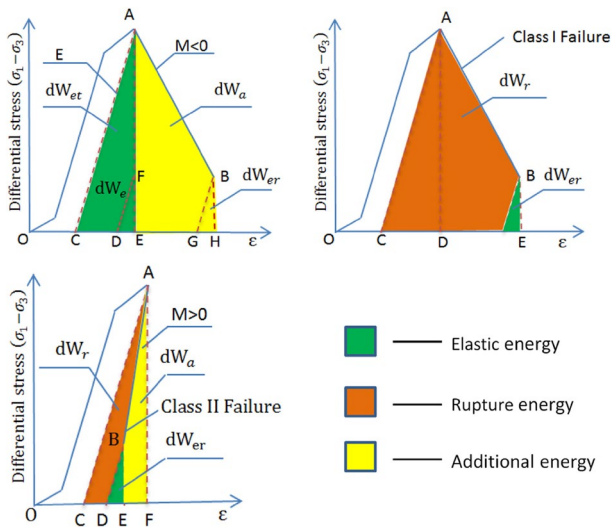


Fig. 1 Post-peak energy balance for Class I and Class II failure on stress–strain curve, Tarasov and Potvin (2013) and Decheng Zhang et al. (2016)

- a) For very good quality hard rock masses, with a high GSI value ($GSI > 75$), the rock mass behavior is elastic brittle.
- b) For averagely jointed rock ($25 < GSI < 75$), the strain softening.
- c) For very weak rock ($GSI < 25$), the rock mass behaves in an elastic perfectly plastic manner (according to Fig. 3).

The brittle and perfectly plastic behaviors are special cases of the strain softening behavior because the strain softening behavior can accommodate brittle and perfectly plastic behaviors (Alejano et al. 2009). The slope for the softening stage or drop modulus is denoted by M . If this parameter tends to infinity, perfectly brittle behavior appears, whereas perfectly plastic behavior is obtained if this modulus tends to zero (Alejano et al. 2009)..

Cai et al. (2007), proposed estimating the residual strength of rock masses by adjusting peak GSI to the residual GSI value by using of two major controlling factors in the

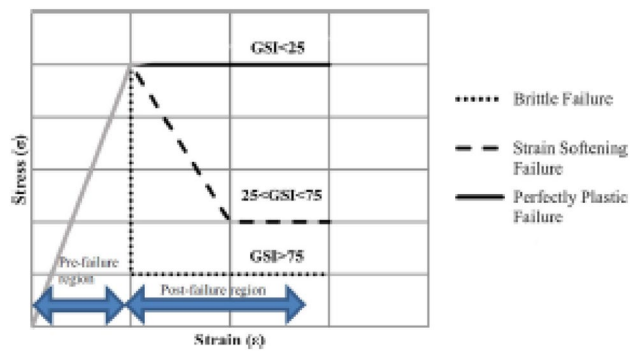


Fig. 3 Different post-failure behavior modes for rock masses (Tutluoğlu et al. 2015)

Table 1 Initial approach to roughly estimating GSI_{res} starting only from the GSI_{peak} (Alejano et al. 2010)

GSI_{peak}	GSI_{res}
75	35–45
70	30–40
60	28–37
50	25–33
40	23–30
30	21–27
25	20–25

GSI system including residual block volume V_{rb} and residual joint condition factor J_{rc} . To obtain Peak failure criterion can be used of GSI_{peak} in Hoek and Brown equations and the residual failure criterion is similarly obtained by changing the value of the peak geotechnical quality GSI_{peak} to that of the residual geotechnical quality GSI_{res} . The guidelines given by Cai et al. (2007) used to estimate GSI_{res} is mentioned in Table 1.

One of the most important parameters affecting the post-peak behavior of rock mass is the confinement stress which affects the rock mass behavior. With the increased confinement stress the rock mass behavior becomes more and more ductile and finally it behaves as ideally plastic (Rummel and Fairhurst 1970) and the drop modulus tends to zero. With

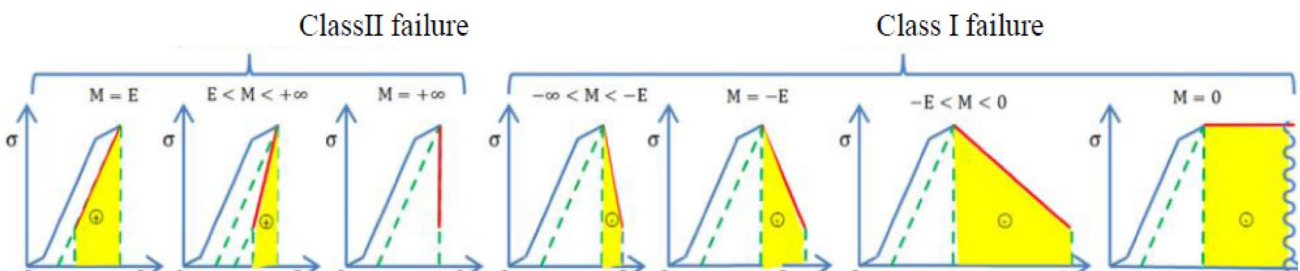


Fig. 2 Two type stress – strain curve of rock mass based on the drop modulus (Class I and Class II failure), Tarasov and Potvin (2013) and Decheng Zhang et al. (2016)

decreased confinement pressure, the rock mass behavior tends to brittle and the drop modulus increases to infinite. The conclusion of Seeber (1999) showed that ideally plastic behavior, without strain softening post failure, may be expected when the confinement pressure σ_3 , is equal to or greater than one-fifth of the axial stress at failure (Egger 2000). It is shown in Fig. 4).

Assuming the Hoek and Brown failure criterion, based on Seeber’s condition, the relation between the confinement

Poisson’s ratio, ν , does not usually affect the rock behavior to a significant degree, so standard values in the range 0.25–0.35 are likely to be valid for any approach (Alejano et al. 2009). As mentioned by Alejano et al. (2009), the value of the drop modulus depends on the deformation’s modulus E_{rm} according to:

$$M = -\omega \cdot E_{rm} \tag{2}$$

The value of the ratio ω depends on the GSI peak and confinement-stress level and can be estimated according to:

$$\omega = \left[0.0046e^{0.0768 \cdot GSI^{peak}} \right] \left(\frac{\sigma_3}{\sqrt{s^{peak}} \cdot \sigma_{ci}} \right)^{-1} \text{ for } \frac{\sigma_3}{\sqrt{s^{peak}} \cdot \sigma_{ci}} \geq 0.1, \tag{3}$$

$$\omega = \left[0.0046e^{0.0768 \cdot GSI^{peak}} \right] \left(\frac{\sigma_3}{2\sqrt{s^{peak}} \cdot \sigma_{ci}} + 0.05 \right)^{-1} \text{ for } \frac{\sigma_3}{\sqrt{s^{peak}} \cdot \sigma_{ci}} \leq 0.1. \tag{4}$$

pressure and the uniaxial compressive strength σ_c , of the intact rock can be obtained (Egger 2000). This relation can be approximated by:

$$\sigma_{3,crit} \geq \frac{\sigma_c \cdot m_b}{16}, \tag{1}$$

where m_b is the product of a parameter m depending on the lithology, with a reduction factor depending on the degree of fracturing of the rock.

As mentioned above it has been observed in the field that the post-failure deformability behavior of rock masses is highly dependent on the rock mass quality, deformation modulus and confinement stress. Based on these observations, the following values proposed by Alejano et al. (2009) to estimate the drop modulus of the rock mass according to the peak rock mass quality given by GSI peak and to the level of confinement stress expressed in terms of the rock mass compressive strength given by $\sqrt{s^{peak}} \cdot \sigma_{ci}$

If the confinement stress is not considered in calculation, the drop modulus can be estimated according to Eq. 5 (Alejano et al. 2009):

$$M = \frac{E_{rm}}{0.08 \cdot GSI - 7} \text{ For } 25 < GSI < 75. \tag{5}$$

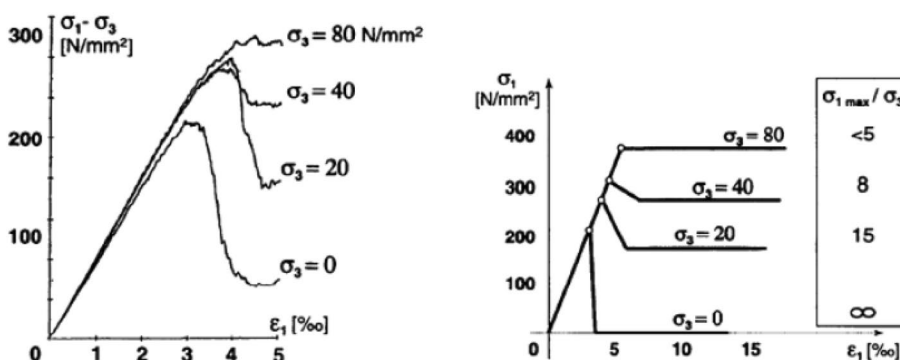
A more complex approach to estimate the drop modulus, including the effect of σ_{ci} is (Alejano et al. 2009):

$$M = \frac{E_{rm}}{0.0812 \left(GSI + \frac{\sigma_{ci}(MPa)}{10} \right) - 7.66} \text{ For } 20 < GSI < 75. \tag{6}$$

The following equation is used as a first approach to estimate the drop modulus, if one uses more complex strain softening models with confinement stress dependent drop modulus (Alejano et al. 2009):

$$M = \frac{1000 \cdot E}{GSI \cdot \sigma_3 + 75 \cdot GSI - 225 \sigma_3 - 5875} \text{ For } 25 < GSI < 75. \tag{7}$$

Fig. 4 Dependence of the post-failure behavior of granite samples on the confinement pressure. **a** Results of a numerical simulation of the 3-axial tests. **b** Schematic behavior (Egger 2000)



The most complex equation to estimate the drop modulus is defined as (Alejano et al. 2009):

$$M = \frac{E_{rm}}{1 - \left[\left[\frac{8.66 - 0.0812 \cdot (GSI + \sigma_{ci}(\text{MPa}))}{8 - 0.08 \cdot GSI} \right] \cdot \left[\left(\frac{225 - GSI}{1000} \right) \cdot \sigma_3 + \left(\frac{55 - 0.6GSI}{8} \right) \right] \right]} \quad (8)$$

The Eq. 8 is used for GSI ranges from 20 to 75 and more effective factors such as GSI, confinement stress, σ_3 , uniaxial strength of intact rock σ_{ci} are applied in this equation (Alejano et al. 2009).

In this paper, the deformation modulus, E_{rm} , can be obtained from Hoek and Diederichs approach due to using more effective factors on deformability such as the elastic modulus of intact rock, E_i , disturbance factor, D , and GSI in this equation (Hoek and Diederichs 2006; Soleiman Dehkordi et al. 2011, 2013, 2015a, 2015b).

$$E_{rm} = E_i \cdot \left(\frac{1 - \frac{D}{2}}{1 + e^{\left(\frac{75 + 25D - GSI}{11} \right)}} \right) \quad (9)$$

All mentioned equations were used to estimate the drop modulus in this paper.

The aim of this work is to estimate the drop modulus using the brittleness index of intact rock and Geological Strength Index of rock mass based on the actual collected data from Nosoud and Zagros Tunnels in Iran.

Brittleness indexes

Brittleness is a comprehensive mechanical properties of rocks. Several definitions of brittleness index were proposed by many authors but there is no agreement between different authors about the definition and measurement methods of

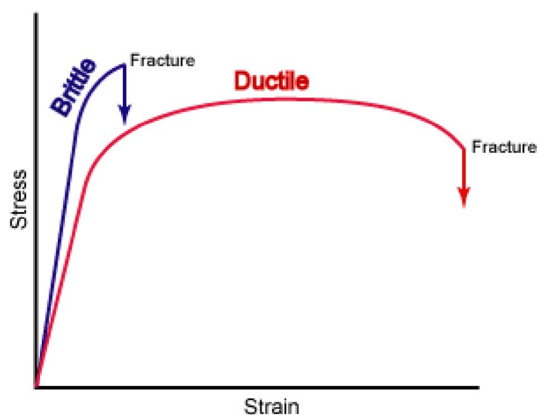


Fig. 5 Graph comparing stress–strain curves for brittle and ductile materials, (Perez and Marfurt 2014)

brittleness. Determination of rock brittleness is not simple because its concept is not standardized. The determination of

brittleness index is largely empirical. Brittleness index was defined by Morley and Hetényi as the lack of ductility. The brittle and ductile behavior of rocks is determined based on the stress–strain curve of rocks as shown Fig. 5, (Perez and Marfurt 2014).

Materials and many rocks usually terminating by fracture at or only slightly beyond the yield stress defined as brittle (Obert and Duvall 1967). Different definitions of brittleness are summarized by Hucka and Das (1974). They also defined a brittleness obtained from load–deformation curves. Ramsay (1967) defines brittleness as follows: ‘‘when the internal cohesion of rocks is broken, the rocks are said to be brittle.’’ It is cleared that increasing the brittleness index can cause to make the following phenomena:

- Low values of elongation of grains;
- fracture failure;
- formation of fines;
- higher ratio of compressive to tensile strength;
- higher resilience;
- higher angle of internal friction;
- formation of cracks in indentation.

The brittleness index is evaluated based on measurements or tests, such as tensile strength and compressional strength test, and hardness measurements. It is applicable to obtain the stress–strain curve which can be used to determine the brittleness.

As Fig. 5 shows, a material is brittle if, when subjected to stress, it breaks without significant deformation. Brittle materials absorb relatively little energy prior to fracture, even those of high strength. Meanwhile, ductility is a solid material’s ability to deform under stress. In elastic region, the relation between the applied stress which is directly proportional and the resulting strain (up to a certain limit) can be explained by a graph in which those two quantities are presented as a straight line (red line). The slope of this line is known as Young’s modulus (E). It can be used to determine the stress–strain relationship in the linear elastic portion of the stress–strain curve. In plastic region, plastic deformation is retained after the release of the applied stress. Most materials in the linear-elastic category are usually capable of plastic deformation. Brittle materials, like ceramics, do not experience any plastic deformation and will fracture under relatively low stress. In literatures of material science, the

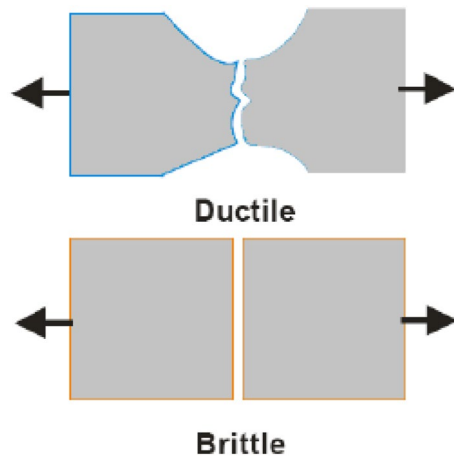


Fig. 6 Brittle and ductile fracturing, Broek (1986) and Nejati and Moosavi (2017)

brittleness calculating methods mainly use tests results/data of rock strengths (compressional strength & tensile strength) or hardness.

Figure 6 schematically depicts the difference between the brittle and ductile fracturing. state of stress and loading rate have substantial influences on the material brittleness, to a large extent, ductility and brittleness depend on the intrinsic characteristics such as mechanical composition and micro-structure, Broek (1986) and Nejati and Moosavi (2017). It should be mentioned that ductile fracturing hardly ever occurs in rocks. The ductile fracturing phenomenon is usually observed in metals, whereas most rocks behave as brittle under the normal conditions. However, not all rocks have the same brittleness value, and rocks can be categorized into different brittleness classes, Nejati and Ghazvinian (2014).

In previous years, some researchers have attempted to correlate brittleness index with other mechanical properties of rocks. For example, brittleness was presented as a function of rock strain by George (1995). Another strain-based

approach is to define brittleness as reversible strain to total strain ratio (Hucka and Das 1974). Hucka and Das (1974) stated that brittleness can be determined from Mohr’s envelope at zero normal stress. Protodyakonov (1963) believed that brittleness values can also be determined from Protodyakonov impact test (Singh 1986).

Yagiz (2009) developed an empirical method as a function of strengths (UCS and BTS) and density of rock to estimate the brittleness index of rocks using the punch penetration test. Further, Yagiz (2009) modified punch penetration test to directly measure rock brittleness. Brittleness index is often determined based on Brazilian tensile strength (BTS) and uniaxial compressive strength (UCS) of rock in engineering practice (Hucka and Das 1974; Singh 1986; Altindag 2002; Kahraman 2002; Gong and Zhao 2007; Heidari et al. 2014). Although a large number of rock brittleness measurement methods have been suggested in the literature, still it has not yet been standardized. What follow, are the three common strength-based approaches to measure the brittleness index of rocks (BI₁–BI₃):

$$BI_1 = \frac{\sigma_c}{\sigma_t}, \tag{10}$$

$$BI_2 = \frac{\sigma_c - \sigma_t}{\sigma_c + \sigma_t}, \tag{11}$$

$$BI_3 = \frac{\sigma_c \cdot \sigma_t}{2}. \tag{12}$$

Equations (10) and (11) have been proposed by Hucka and Das (1974) and Altindag (2002) has presented Eq. (12). where BI₁, BI₂ and BI₃ is the brittleness Indexes determined from compressive and tensile strength, σ_c is the uniaxial compressive strength and σ_t is the tensile strength. As it may be seen in Fig. 7, in general, brittleness indices, BI₁ and BI₂ are not able to describe a scale of brittleness with

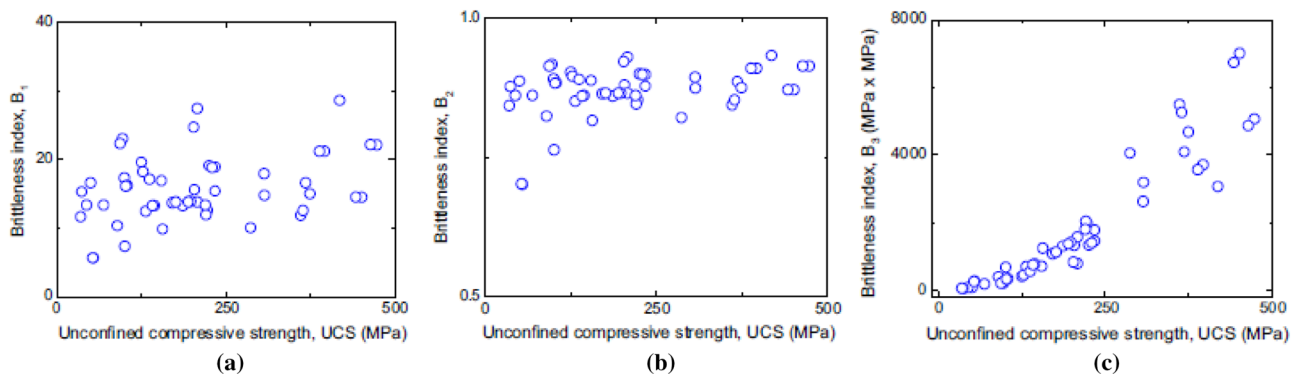


Fig. 7 Relations between compressive-to-tensile brittleness indices **a** BI₁, **b** BI₂ and **c** BI₃ with unconfined compressive strength. Data from Literature (Howarth 1987; Paone et al. 1969; Munoz et al. 2016)

Table 2 Summary of current brittleness index definitions, generated by Decheng Zhang et al. (2016)

Formulae	Variable	Test method
$BI_1 = \varepsilon_{el}/\varepsilon_{tot}$	ε_{el} and ε_{tot} are elastic and total strain at failure	Stress Strain test
$BI_2 = W_{el}/W_{tot}$	W_{el} and W_{tot} are elastic and total energy at failure	
$BI_3 = \varepsilon_{li} * 100\%$	ε_{li} is absolute irreversible longitudinal strain at failure	
$BI_4 = \frac{\tau_p - \tau_r}{\tau_p}$	τ_p and τ_r refer to the peak and residual shear strengths	
$BI_5 = \frac{\varepsilon_f^p - \varepsilon_c^p}{\varepsilon_c^p}$	ε_f^p and ε_c^p refer to the Plastic strains at which the friction strength if fully mobilized and the cohesive strength reduces to the residual value	
$BI_6 = \frac{E_n - \nu_n}{2}$	E_n and ν_n are normalized young's modulus and poissions ratio	
$BI_7 = \frac{E}{\nu}$	E is young's modulus ν is poisson's ratio	
$BI_8 = \frac{E}{\rho}$	ρ is density	
$BI_9 = \frac{M-E}{M}$	E is the unloading elastic modulus	
$BI_{10} = \frac{E}{M}$	M is the post-peak elastic modulus	
$BI_{11} = \sigma_c/\sigma_t$	σ_c , σ and σ_t are unconfined compressive strength and tensile strength respectively	
$BI_{12} = \frac{\sigma_c - \sigma_t}{\sigma_c + \sigma_t}$	ρ is density	
$BI_{13} = \sigma_c \sigma_t / 2$		UCS and Brazilian tensile
$BI_{14} = 0.198 \sigma_c - 2.174 \sigma_t + 0.913 \rho - 3.807$		
$BI_{15} = \frac{F_{max}}{P}$	F_{max} : Maximum applied force P : corresponding penetration at F_{max}	Punch Penetration test
$BI_{16} = q\sigma_c$	σ_c : uniaxial compressive strength q percentage of fines (< 0.6mm in diameter)	Proto-dyakovon impact test
$BI_{17} = \frac{H_\mu - H}{K}$	H_μ and H are the micro and macro indentation hardness K is the bulk modulus	Hardness test
$BI_{18} = \frac{Q}{Q+C+Cl}$	Q Quartz C carbonate	Mineralogical logging or XRD
$BI_{19} = \frac{Q+Dol}{Q+Dol+Lm+Cl+TOC}$	Cl clay Dol dolomite Lm limestone	
$BI_{20} = \frac{W_{QFM} + W_{Carb}}{W_{tot}} \approx \frac{W_{QFM} + W_{calcite} + W_{dolomite}}{W_{tot}}$	TOC total organic content W_{QFM} : weight of quartz, feldspar and mica W_{carb} : weight of carbonate minerals including dolomite, calcite and other carbonate mineral W_{tot} : weight of total minerals	
$BI_{21} = -1.8748 * \phi + 0.9679$	ϕ is the internal friction angle	Lab test or well log data
$BI_{22} = \sin \theta$	θ is the internal friction angle	
$BI_{23} = OCR^b = \left(\frac{\sigma'_v \max}{\sigma'_v} \right)^b$	OCR : over-consolidation ratio b : empirical constant $\sigma'_v \max$ and σ'_v are maximum effective vertical stress it has experienced and the current effective vertical stress	
$BI_{24} = \frac{\lambda}{\lambda + 2\mu}$	λ is lame's first parameter μ is shear modulus	
$BI_{25} = \frac{E}{\lambda}$	E is Young's modulus	

rock compressive strength increasing, i.e. a soft rock may have the same brittleness BI_1 and BI_2 as a hard rock but BI_3 shows a better correlation with the behavior of rock mass (Altindag 2009; Altindag and Guney 2010; Munoz et al. 2016).

Several equations were proposed to estimate the brittleness index and it was briefly shown in Table 2 (Decheng Zhang et al. 2016).

The aim of this work is to propose the drop modulus using the brittleness indexes (Eqs. 10–12) and geological strength index of rock mass, GSI, based on the actual collected data from Nosoud and Zagros tunnels in Iran.



Fig. 8 Location of study area in Iran (red line is the tunnel route) (Sahel Consulting Eng., SCE 2011; Fatemi Aghda et al. 2016)

Project description and geology

In this section, engineering geology and characteristics of Nosoud and Zagros tunnels of Iran is described respectively.

Nosoud tunnel

Nosoud tunnel with a length of 14 km and 4.5 m diameter is located in Kermanshah Province of Iran (Fig. 8).

According to the Nogole-Sadat and Almasian's (1988) division, the study area is a part of two geological zones: Zagros Folded Belt and Northern Zagros thrust. Major fault zones along the tunnels are located in Zagros Folded Belt zone (more than 95%) and a small section at the end of the tunnel route is located in the Northern Zagros zone. Rock formation in the study area includes a collection of sedimentary rocks consisting of limestone, argillaceous, and shale deposited during a long time period (Jurassic-Cretaceous). The profile of geology and geological map of Nosoud tunnel is presented in Fig. 9 (Fatemi Aghda et al. 2016).

Ten sections of engineering geology can be seen along the route of tunnel. Some intact rock and rock mass properties characterization as well as rock mass classifications such as rock mass rating, RMR (Bieniawski 1989), quality system, Q , (Barton et al. 1974) and geological strength index, GSI, (Hoek 1994) systems were performed on the engineering geological units of Nosoud tunnel (Table 3).

Five types of rock masses were identified along the tunnel alignment: (a) Type 1: layered and jointed alternation of thin-bedded limestone and shale with massive limestone which constitutes 59% of the tunnel length. (b) Type 2:

massive to blocky dark gray limestone which constitutes 8.5% of the tunnel length. (c) Type 3: layered and jointed alternation of thin-bedded limestone with shale which constitutes 18% of the tunnel length. (d) Type 4: layered and jointed dark gray thin-bedded limestone which constitutes 11% of the tunnel length. (e) Type 4-1: faulted thin-bedded limestone which constitutes 3.5% of the tunnel length. Formations including J1Kh, J4Kh, J5Kh, and Kgr were identified with a high quantity of shale and argillaceous limestone. In addition, J2Kh, J3Kh, J6Kh, K^a bg, and Kbg formations consist of a high percentage of lime and their strength is higher than shale and argillaceous limestone (Fatemi Aghda et al. 2016).

Zagros tunnel

Zagros long tunnel (lot 2) with a length of 26 km and about 6.73 m diameter is located in Kermanshah Province in the west of Iran (Fig. 10).

This tunnel has been designed to transfer water (maximum discharge of 64.4 m³/s) from the Sirwan River to the tropical plains such as the Zohab plain. According to 1:100,000 Geological Map of Kermanshah (KarimiBavandpur and HajiHoseini 1990) (Fig. 10), geological formations in the tunnel route are Jurassic units (Ilam Formation), Cretaceous limestone units, Gurpi Formation, Garu Formation, Khami Group, and Pabdeh Formation (Fig. 11).

These formations mainly consist of dark gray shale, shaly limestone, and limestone rocks. The study area is located in the Zagros Fold Thrust Belt (Berberian 1995). Arabian plate compressional tectonic forces have created several faults and thrust faults with NW-SE trend in the study area. The tunnel strike is NESW, so that cuts vertically the trend of region structures. Based on some characteristics such as lithology of layers, differences of structural features and geotechnical characteristics, 16 engineering geology units have been distinguished in the study area (Table 4).

To study of strength properties of rock masses, a number of boreholes were drilled. Also, several core and block samples were selected for laboratory studies. Some of the geotechnical characteristics of intact rock to evaluate brittleness are presented in Table 5.

Data analysis

Rock mass classifications such as RQD, Q and GSI systems have been performed in Nosoud and Zagros tunnels (according to Tables 3, 4). Also, some of the geotechnical characteristics of intact rock to evaluate the brittleness index in Nosoud and Zagros tunnels are respectively presented in Tables 3 and 5. The data obtained from Sahel and Imensazan Consulting Engineers Companies 2008. As mentioned above the drop modulus is a function of several parameters such as

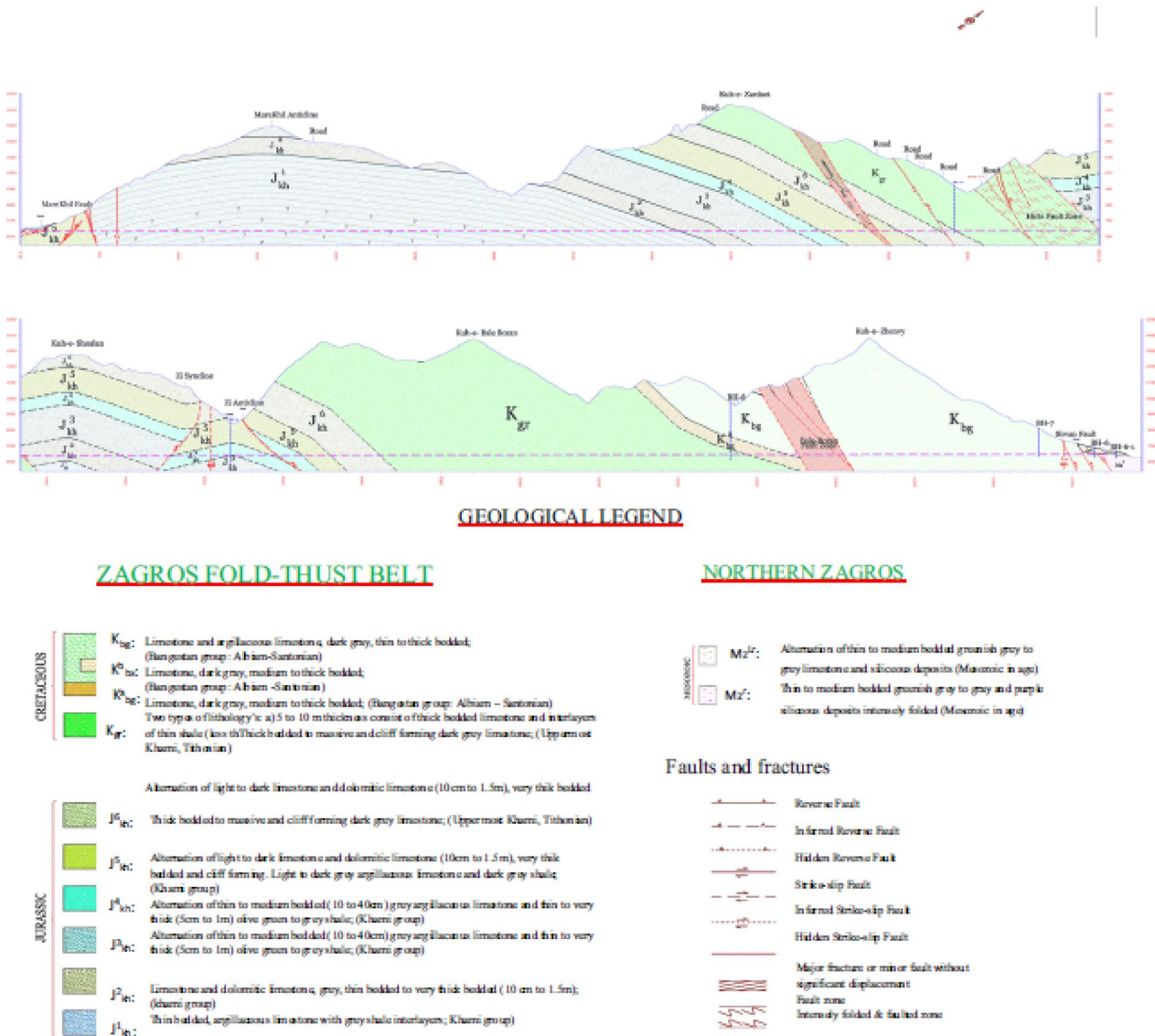


Fig. 9 Geology of the tunnel area and a longitudinal geological section along the tunnel (Sahel Consulting Eng. 2010, Fatemi Aghda et al. 2016)

intact rock properties, quality of rock mass and confinement stress. The calculation of brittleness values and generation of the plots were done by the authors.

Estimation of the drop modulus in Nosoud and Zagros Tunnels using the brittleness indexes

The main purpose of this section is to predict the drop modulus using the brittleness indexes in Nosoud and Zagros tunnels. For this reason, 69 and 27 sections in different zones of Nosoud and Zagros tunnels were respectively considered and estimation of the drop modulus, M , was conducted using actual information of mentioned tunnels. The regression

analysis is used to investigate the kind of relations between M and BI_1 , BI_2 and BI_3 without considering the post-failure behavior of rock mass. As illustrated in Figs. 12, 13 and 14, there are no clear relations between M and BI_1 and BI_2 in any tunnel and a direct relation between M and BI_3 is achieved in Nosoud and Zagros tunnels. It is cleared that the maximum correlation between the drop modulus and the brittleness indexes is obtained using BI_3 index to estimate the drop modulus (as shown in Table 6). As mentioned above the drop modulus is related to the rock mass conditions such as quality of rock mass, confinement stress and etc. By reason, in the next section, the relation between the drop modulus with the brittleness index of intact rock and GSI, as index

Table 3 Intact rock, rock mass properties and rock mass classifications (Sahel Consulting Eng., SCE 2011; Fatemi Aghda et al. 2016)

Engineering geological units	Dry density (kN/m ³)	Saturated density (KN/m ³)	Elastic modulus (kN/m ²)	Poisson ratio	Cohesion (kN/m ²)	Internal friction angle	Dilatation angle	Porosity (%)	Permeability (m/s)	Q	GSI
J_1^{KH}	25	26	1.35×10^7	0.25	0	30	0	10	1×10^7	3.5	45
J_2^{KH}	26	26.5	2×10^7	0.25	0	30	0	10	1×10^7	2	37
J_3^{KH}	26	26.5	1.45×10^7	0.210	0	30	0	3	1×10^7	2.4	50
J_4^{KH}	25	25.5	1.15×10^7	0.13	0	30	0	7.5	1×10^7	2.25	37
J_5^{KH}	27	27.5	4×10^6	0.270	0	30	0	3	1×10^7	2	40
J_6^{KH}	27	27.5	1×10^7	0.240	0	30	0	1.25	1×10^7	2.75	47
Kgr	25	25.5	2.60×10^7	0.1	5	35	0	4	1×10^7	2.55	42
Kbg	26	26.5	3×10^7	0.1	0	30	0	4.5	1×10^7	1.8	45
K_{bg}^a	25	26	2×10^7	0.1	0	35	0	1.25	1×10^7	4.5	50
MZ^a	26	26.5	3.50×10^6	0.25	0	30	0	1.5	1×10^7	0.75	35
M.F.Z	27	27.5	1×10^7	0.24	0	30	0	8	1×10^7	0.5	32.5
B.B.F	26	26.5	2×10^7	0.25	0	30	0	7.5	1×10^7	0.5	30

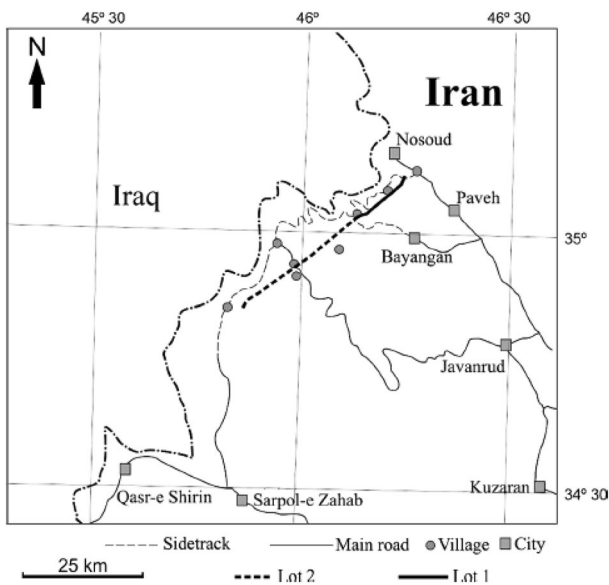


Fig. 10 Location map of the study area (Sahel and Imensazan Consulting Engineers Companies 2008)

parameter to estimate the quality of rock mass, is simultaneously investigated in any tunnel.

Estimation of the drop modulus in Nosoud and Zagros Tunnels using the brittleness indexes of intact rock and quality of rock mass

As mentioned above, the drop modulus parameter is highly related to the quality of rock mass and there is a direct

relation between both parameters. It was cleared that increasing the quality of rock mass can cause to increase the brittleness index because the post-peak behavior is brittle and it is true inversely. In the previous section, it was shown that BI_3 is the best parameter to estimate the drop modulus so it is used in this section. Also, the classification of rock mass is done by using of GSI and all rock masses of both tunnels was classified in the average class and the post-peak behavior of rock mass is assumed strain—softening. As shown in Fig. 15, there is a direct relation between the drop modulus with $\left(\frac{BI_3 \cdot GSI}{100}\right)$ and the maximum correlation was respectively achieved using the power and exponential equations in Nosoud and Zagros tunnels to estimate the mentioned parameter. Based on the regression analysis, it is cleared that the correlation coefficient of new proposed equations in any tunnel is better than the previous mentioned equations (according to Table 7).

Estimation of the drop modulus using the brittleness indexes of intact rock and the geological strength index of rock mass

In this section, in the first step, estimation of the drop modulus is accrued using the brittleness indexes of intact rock of mentioned tunnels. The regression analysis was applied to find the best relation between mentioned parameters. As shown in Fig. 16, the relation between both parameters is direct and the best correlation between them was achieved using the polynomial equation to estimate the drop modulus (according to Table 8).

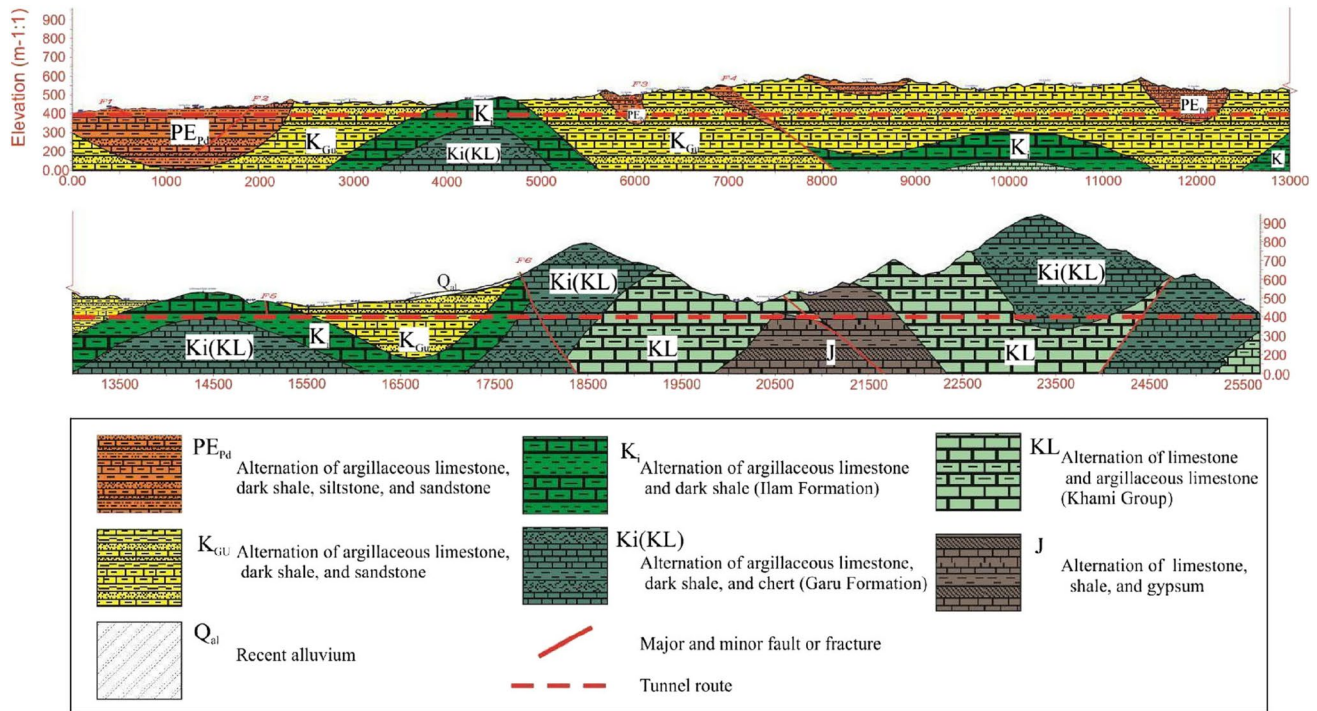


Fig. 11 Longitudinal geological profile of Zagros long tunnel, (Sahel and Imensazan Consulting Engineers Companies 2008)

Table 4 The estimated rock mass classification systems (Sahel and Imensazan Consulting Engineers Companies, SCE 2008 and ICE 2008)

Engineering geology unit	Lithology	Rock mass classification systems			
		RQD (%)	RMR	GSI	<i>Q</i>
SH-ML1	Shale, marly limestone	70	48	40	3.25
SH-ML3	Shale, marly limestone	60	44	43	2.2
ML-SH2	Marly limestone	65	48	47	2.7
ML-SH3	Dark marly limestone and shale	60	46	40	2.5
ML-SH4	Shale, marly limestone	70	50	43	3.9
ML-SH5	Shale, marly limestone	80	65	50	5.8
SH-LS1	Shale, limly shale	60	40	37	2.75
SH-LS2	Shale, limly shale	60	50	44	2.7
SH-LS4	Shale, shaly, limestone, sandstone	75	48	43	1.94
L12	Limestone, shaly limestone	85	57	57	4.68
L13	Limestone	87	57	58	5.63
L14	Limestone	72	50	44	2.34
L15	Limestone	84	54	50	5.31
LI-MA	Limestone, marl	68	41	38	1.46
LI-SH	Limestone, shale, gypsum	65	42	48	2.71
L16	Limestone	95	66	60	11.88

Finally, based on the actual collected data from both mentioned tunnels, the relation between the drop modulus with $\left(\frac{BI_3 \cdot GSI}{100}\right)$ is reviewed and the next polynomial equation is

achieved between them (according to Fig. 17). As shown in Table 8, The most useful equation to estimate the drop modulus was achieved using the BI_3 and GSI because it is a function of both parameters.

Table 5 Average values of physico-mechanical properties of the tunnel route rocks (Sahel and Imensazan Consulting Engineers Companies, SCE 2008 and ICE 2008)

Engineering geology unit	<i>N</i> (%)	<i>P</i> (KN/m ³)	BTS (MPa)	UCS (MPa)	<i>E</i> (GPa)
SH-ML1	12.10	24.03	2.25	22.5	5.00
SH-ML3	12.50	23.54	1.50	15.0	5.05
ML-SH2	7.50	23.05	2.30	22.5	5.75
ML-SH3	7.80	22.07	3.00	37.5	5.70
ML-SH4	8.00	22.56	3.00	22.5	4.95
ML-SH5	4.00	23.54	5.00	75.0	6.25
SH-LS1	7.50	24.03	2.00	22.5	5.10
SH-LS2	8.50	23.54	3.00	40.0	5.50
SH-LS4	7.50	24.03	3.50	37.5	5.00
L12	3.50	24.72	4.25	120.0	22.5
L13	2.30	25.02	7.50	125.0	14.0
L14	2.30	25.21	4.25	75.0	7.50
L15	10.00	24.03	4.25	62.5	7.30
LI-MA	2.50	21.58	2.00	42.5	3.50
LI-SH	2.55	24.53	2.00	37.5	3.60
L16	3.00	24.03	7.50	11.5	22.1

Conclusion

In this research, the following results were obtained

1. The best correlation between parameters was achieved when Eqs. 2–4 were used to estimate the drop modulus.
2. Based on the statistical analysis, it becomes apparent that there are no clear relations between *M* with BI₁ and BI₂ in any tunnel. Also there is a direct relation between the drop modulus and BI₃.
3. The classification of rock mass is done by using of GSI classification and all rock masses of both tunnels was classified in the average class and the post-peak behavior of rock mass is assumed strain-softening.
4. The result shows that there is a direct relation between the drop modulus with $\left(\frac{BI_3 \cdot GSI}{100}\right)$ and the maximum correlation was respectively achieved using the power and exponential equations in Nosoud and Zagros tunnels to estimate the mentioned parameter.
5. The most useful equation to estimate the drop modulus was achieved using the BI₃ and GSI Simultaneously because it is a function of both parameters.

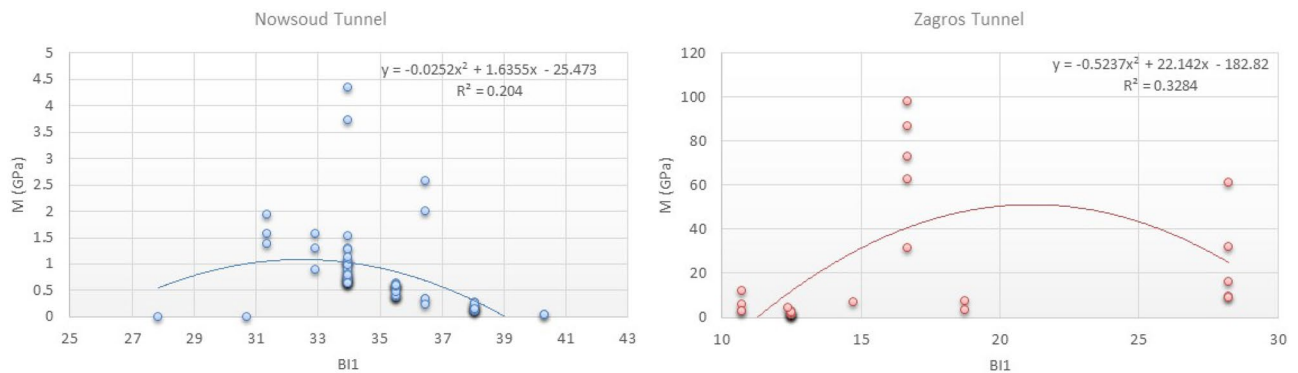


Fig. 12 The relations between the drop modulus and BI₁ in Nosoud and Zagros tunnels of Iran

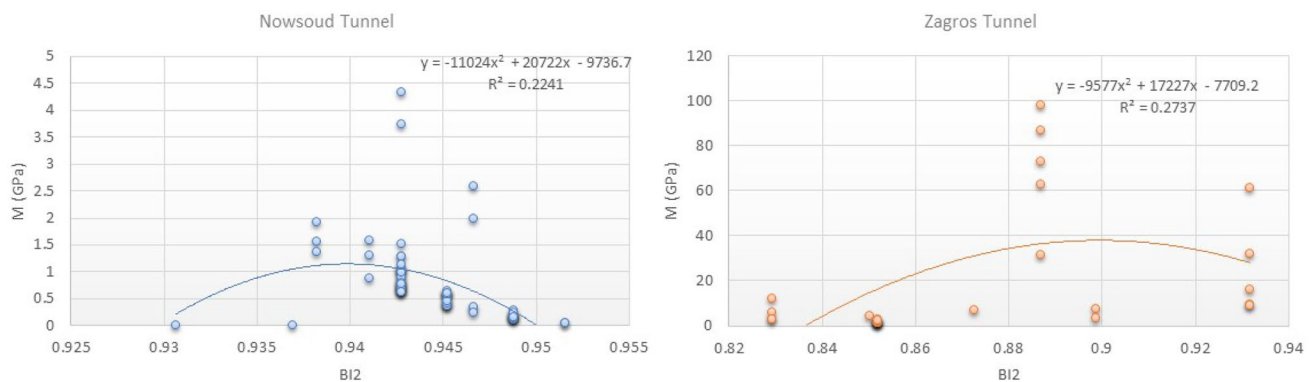


Fig. 13 The relations between the drop modulus and BI₂ in Nosoud and Zagros tunnels of Iran

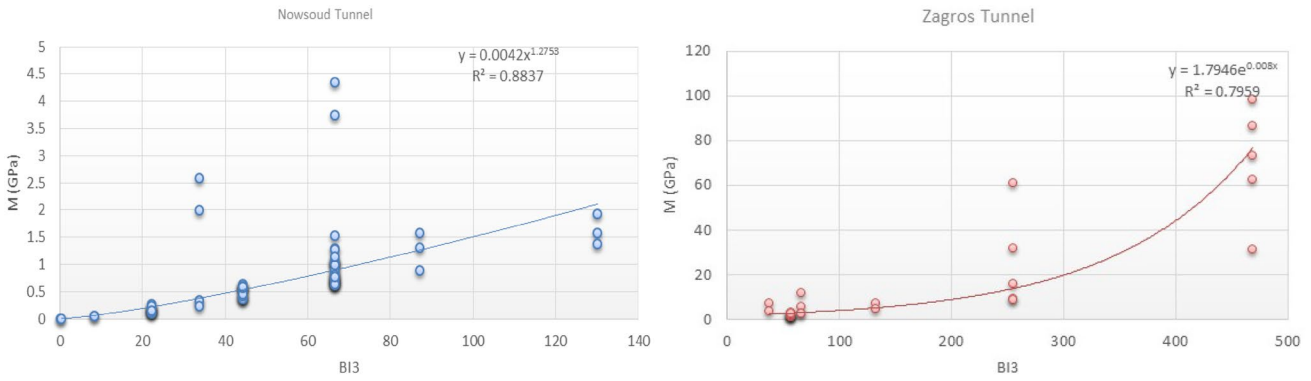


Fig. 14 The relations between the drop modulus and BI₃ in Nosoud and Zagros tunnels of Iran

Table 6 The proposed relations between the drop modulus and Brittleness indexes in Nosoud and Zagros tunnels of Iran

Tunnel name	Proposed equations to estimate M using BI_1 R^2	Proposed equations to estimate M using BI_2 R^2	Proposed equations to estimate M using BI_3 R^2
Nowsoud	$M = -0.0252BI_1^2 + 1.6355BI_1 - 25.473$ 0.204	$M = -11024BI_2^2 + 20722BI_2 - 9736.7$	$M = 0.0042BI_3^{1.2753}$ 0.2241 0.8837
Zagros	$M = -0.5237BI_1^2 + 22.142BI_1 - 182.82$ 0.3284	$M = -9577BI_2^2 + 17227BI_2 - 7709.2$	$M = 1.7946e^{0.008BI_3}$ 0.2737 0.7959

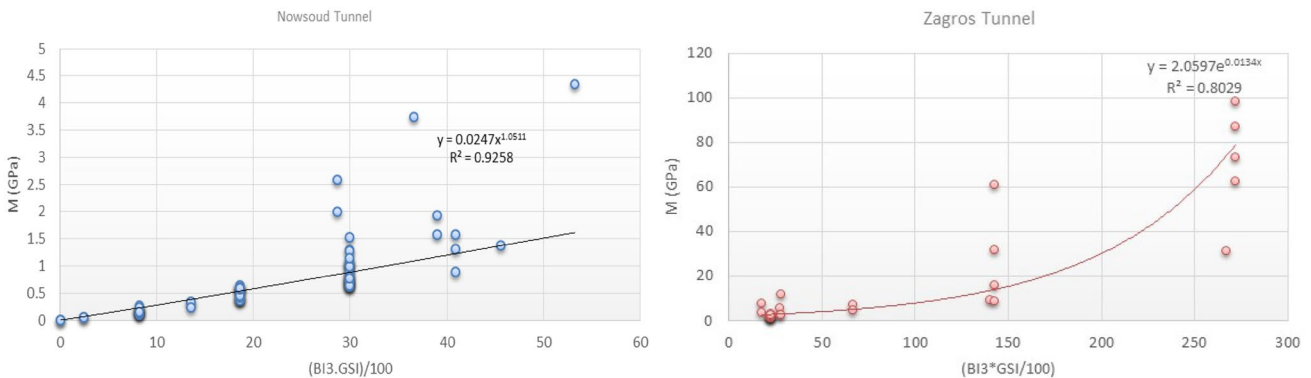


Fig. 15 The relation between the drop modulus with BI₃ and GSI in Nosoud and Zagros tunnels of Iran

Table 7 The proposed equations to estimate the drop modulus using the Brittleness indexes of intact rock and the geological strength index of rock mass in Nosoud and Zagros tunnels of Iran

Tunnel name	Proposed equations with $\left(\frac{BI_3 \cdot GSI}{100}\right)$ R^2
Nowsoud	$M = 0.0247\left(\frac{BI_3 \cdot GSI}{100}\right)^{1.0511}$ 0.9258
Zagros	$M = 2.0579e^{0.0134\left(\frac{BI_3 \cdot GSI}{100}\right)}$ 0.8029

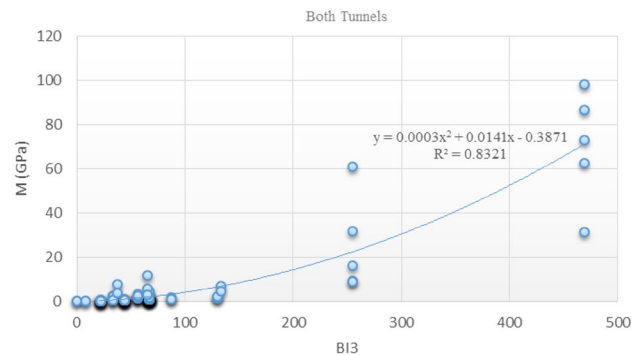


Fig. 16 The relation between the drop modulus with BI₃ in Both tunnels of Iran

Table 8 the proposed equations to estimate the drop modulus using the Brittleness indexes of intact rock and using $\left(\frac{BI_3 \cdot GSI}{100}\right)$

Relation types	Proposed equations
Relation between the drop modulus and BI_3	$M = 0.0003BI_3^2 + 0.0141BI_3 - 0.3871$ 0.8321
Relation between the drop modulus and $\left(\frac{BI_3 \cdot GSI}{100}\right)$	$M = 0.0008\left(\frac{BI_3 \cdot GSI}{100}\right)^2 + 0.0611\left(\frac{BI_3 \cdot GSI}{100}\right) - 0.5985$ 0.8417

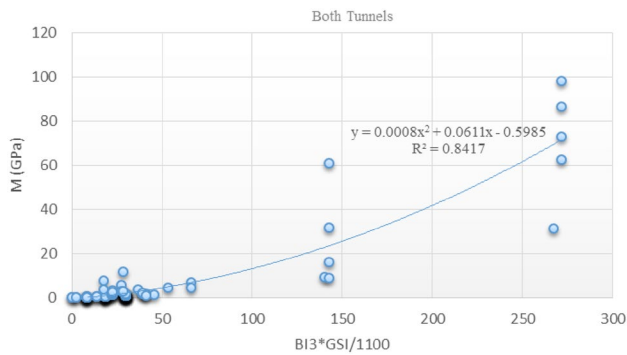


Fig. 17 The relation between the drop modulus with BI_3 and GSI in both tunnels of Iran

6. Finally, based on collected information from both tunnels, the relation between the drop modulus and two indexes such as BI_3 and $\left(\frac{BI_3 \cdot GSI}{100}\right)$ is investigated. The results show a stronger correlation between the drop modulus and $\left(\frac{BI_3 \cdot GSI}{100}\right)$, because the correlation coefficients of the mentioned equation is higher than other equation (proposed equation using BI_3).

References

Alejano LR, Rodriguez-Dono A, Alonso E, Fdez-Manin G (2009) Ground reaction curves for tunnels excavated in different quality rock masses showing several types of post-failure behavior. *Tunn Undergr Sp tech* 24(6):689–705

Alejano LR, Alonso E, Rguez-Dono A, Fdez-Manin G (2010) Application of the convergence-confinement method for tunnel excavated in rock masses exhibiting Hoek-Brown strain-softening behavior. *Int J Rock Mech Min Sci* 47(1):150–160

Altindag R (2002) The evaluation of rock brittleness concept on rotary blast hole drills. *J S Afr Inst Min Metall* 102:61–66

Altindag R (2009) Assessment of some brittleness indexes in rock-drilling efficiency. *Rock Mech Rock Eng* 43:361–370. <https://doi.org/10.1007/s00603-009-0057-x>

Altindag R, Guney A (2010) Predicting the relationships between brittleness and mechanical properties (UCS, TS and SH) of rocks. *Sci Res Essays* 5(16):2107–2118

Barton N, Lien R, Lunde I (1974) Engineering classification of rock masses for the design of tunnel supports. *Rock Mech* 6(4):189–239

Bieniawski ZT (1989) *Engineering rock mass classifications*. Wiley, New York

Brady BHG, Brown ET (2005) *Rock mechanics: for underground mining*, 3rd edn. Springer, Netherlands. <https://doi.org/10.1007/978-1-4020-2116-9>

Broek D (1986) *Elementary engineering fracture mechanics*. Martinus Nijhoff Publishers, Dordrecht

Cai M, Kaiser PK, Tasakab Y, Minami M (2007) Determination of residual strength parameters of jointed rock masses using the GSI system. *Int J Rock Mech Min Sci* 44(2):247–265

Egger P (2000) Design and construction aspects of deep tunnels (with particular emphasis on strain softening rocks). *Tunn Undergr Sp Tech* 15(4):403–408

Fatemi Aghda SM, Ganjalipour. K, Esmaeil Zadeh M (2016) Comparison of squeezing prediction methods: a case study on Nowsoud tunnel. *Geotech Geol Eng* 34:1487–1512. <https://doi.org/10.1007/s10706-016-0056-0>

Gong QM, Zhao J (2007) Influence of rock brittleness on TBM penetration rate in Singapore granite. *Tunn Undergr Space Technol* 22(3):317–324

Heidari M, Khanlari G, Torabi-Kaveh M, Kargarian S, Saneie S (2014) Effect of porosity on rock brittleness. *Rock Mech Rock Eng* 47(2):785–790

Hoek E (1994) Strength of rock and rock masses. *ISRM News J* 2(2):4–16

Hoek E, Brown ET (1997) Practical estimates of rock mass strength. *Int J Rock Mech Sci Geom Abstr* 34(8):1165–1186

Hoek E, Diederichs MS (2006) Empirical estimation of rock mass modulus. *Int J Rock Mech Min Sci* 43(2):203–215

Howarth D (1987) The effect of pre-existing microcavities on mechanical rock performance in sedimentary and crystalline rocks. *Int J Rock Mech Min Sci Geomech Abstr* 4:223–233

Hucka V, Das B (1974) Brittleness determination of rocks by different methods. *Int J Rock Mech Min Sci Geomech Abstr* 11(10):389–392

Imensazan Consulting Engineers Companies/Imensazan Consulting Engineers Company (ICE) (2008) *Engineering geology maps and site reports of Zagros tunnel*

Kahraman S (2002) Correlation of TBM and drilling machine performances with rock brittleness. *Eng Geol* 65:269–283. [https://doi.org/10.1016/S0013-7952\(01\)00137-5](https://doi.org/10.1016/S0013-7952(01)00137-5)

Karimi Bavand pour AR, Haji Hoseini A (1990) *Geological Map of Kermanshah, Scale 1:100000*. GSI

Munoz H, Taheri A, Chanda E (2016) Fracture energy-based brittleness index development and brittleness quantification by pre-peak strength parameters in rock uniaxial compression. *Rock Mech Rock Eng*. <https://doi.org/10.1007/s00603-016-1071-4>

Nejati HR, Ghazvinian A (2014) Brittleness effect on rock fatigue damage evolution. *Rock Mech Rock Eng* 47(5):1839–1848

Nejati HR, Moosavi SA (2017) A new brittleness index for estimation of rock fracture toughness. *J Min Env* 8(1):83–91. <https://doi.org/10.22044/jme.2016.579>

- Nogole-Sadat MAA, Almasian M (1993) Tectonic map of Iran, Scale 1:1,000,000. Geological Survey of Iran
- Obert L, Duvall W (1967) Rock Mechanics and the design of structures in rock. Wiley, New York
- Paone J, Madson D, Bruce WE (1969) Drillability studies: laboratory percussive drilling. Bureau of Mines. Twin Cities Mining Research Center, Twin Cities
- Perez R, Marfurt K (2013) Brittleness estimation from seismic measurements in unconventional reservoirs: application to the Barnett Shale: 83rd A Ann. In: Internat Mtg., Soc. of Expl. Geophys., Expanded Abstract, pp 2258–2263
- Perez Altamar R, Marfurt K (2014) Mineralogy-based brittleness prediction from surface seismic data: application to the Barnett Shale. Interpretation 2(4):T255–T271
- Protodyakonov MM (1963) Mechanical properties and drillability of rock. In: Proceedings of the 5th symposium rock mechanics. University of Minesota, Pergamon Press, New York, pp 103–118
- Ramsay JG (1967) Folding and fracturing of rocks. McGrawHill, London
- Rummel F, Fairhurst C (1970) Determination of the post-failure behavior of brittle rock using a servo-controlled testing machine. Rock Mech 2:189–204
- Sahel Consulting Engineers CompaniesImensazan Consulting Engineers Company (SCE) (2008) Engineering geology maps and site reports of Zagros tunnel
- Sahel Consulting Engineers CompaniesImensazan Consulting Engineers Company (SCE) (2011) Engineering geology maps and site reports of Zagros Tunnel
- Seeber G (1999) Druckstollen und Druckschächte: Bemessung—Konstruktion—Ausführung, ENKE im Georg Thieme Verlag, Stuttgart, New York 1999
- Singh SP (1986) Brittleness and the mechanical winning of coal. Min Sci Technol 3:173–180
- Soleiman Dehkordi M, Shahriar K, Maarefvand P, Gharouninik M (2011) Application of the strain energy to estimate the rock load in nonsqueezing ground condition. Arch Min Sci 56(3):551–566
- Soleiman Dehkordi M, Shahriar K, Maarefvand P, Gharouninik M (2013) Application of the strain energy to estimate the rock load in squeezing ground condition of Emamzade Hashem tunnel in Iran. Arab J Geosci 6(4):1241–1248
- Soleiman Dehkordi M, Lazemi HA, Shahriar K, Soleiman Dehkordi M (2015a) Estimation of the rock load in non-squeezing ground condition using the post failure properties of rock. Mass Geotech Geol Eng 33(4):1115–1128
- Soleiman Dehkordi M, Lazemi HA, Shahriar K (2015b) Application of the strain energy ratio and the equivalent thrust per cutter to predict the penetration rate of TBM, case study: Karaj—Tehran water conveyance tunnel of Iran. Arab J Geosci 8(7):4833–4842
- Tarasov B, Potvin Y (2013) Universal criteria for rock brittleness estimation under triaxial compression. Int J Rock Mech Min Sci 59:57–69
- Tutluoğlu L, Öge İF, Karpuz C (2015) Relationship between pre-failure and post-failure mechanical properties of rock material of different origin. Rock Mech Rock Eng 48(1):121–141. <https://doi.org/10.1007/s00603-014-0549-1>
- Wawersik W, Fairhurst C (1970) A study of brittle rock fracture in laboratory compression experiments. Int J Rock Mech Min Sci Geomech Abstr 7(5):561–575
- Yagiz S (2009) Assessment of brittleness using rock strength and density with punch penetration test. Tunn Undergr Space Technol 24(1):66–74
- Zhang D, Ranjith n PG, Perera MSA (2016) The brittleness indices used in rock mechanics and their application in shale hydraulic fracturing: a review. J Petrol Sci Eng 143:158–170

Publisher's Note Springer Nature remains neutral with regard to jurisdictional claims in published maps and institutional affiliations.